Investigation of Quinquethiophene Derivatives with Different End Groups for High Open Circuit Voltage Solar Cells

Guankui Long, Xiangjian Wan, Bin Kan, Yongsheng Liu, Guangrui He, Zhi Li, Yawei Zhang, Yi Zhang, Qian Zhang, Mingtao Zhang, and Yongsheng Chen**

Three quinquethiophene derivatives with different end groups of octyl 2-cyanoacetate (DCAO5T), 3-ethylrhodanine (DERHD5T) and 2*H*-indene-1,3-dione (DIN5T) are synthesized in order to obtain higher open circuit voltage (V_{oc}) than their septithiophene analogs. The photovoltaic performance of these three molecules as donors and fullerene derivatives as the acceptors in bulk heterojunction solar cells are studied by using the simple solution spin-coating fabrication process. Among them, DERHD5T shows V_{oc} as high as 1.08 volt and power conversion efficiency of 4.63% under AM 1.5G irradiation (100 mW cm^{-2}). The reasons for the high V_{oc} were investigated by the theoretical simulations and consistent results have been obtained in comparison with experimental measurements.

1. Introduction

The performance of organic photovoltaic (OPV) has increased dramatically recently[1–6] and power conversion efficiency (PCE) of 9.2%[7] has been achieved for polymer based solar cells (PSCs) with bulk heterojunction (BHJ) architecture. Meanwhile, small molecule based OPV has also stimulated great attention, owing to its well-defined structures, less batch to batch variation, easier purification and energy structure control compared with the PSCs.[8–18] Nowadays, PCEs over 7%[19–21] have been achieved for small molecule bulk heterojunction (SM BHJ) solar cells, which is close to the performances of the best PSCs.

Oligothiophenes, including one dimensional (1D), 2D and 3D conjugated systems, are one of the largest families of organic semiconductors, and have been widely used in OPVs due to their good transport properties, high polarizability, as well as tunable optical and electrochemical properties.[4–6,22] Our group has synthesized a series of septithiophenes (**O7T**) with different end groups, such as dicyanovinyl (**DCN7T**),[23] alkyl cyanoacetate (**DCAO7T**),[24] 3-ethylrhodanine (**DERHD7T**)[25] et al, with PCE of 3.7%, 5.08% and 6.1%, respectively (as shown in **Figure 1**), indicating that oligothiophenes with electron-withdrawing and/or dye end groups are very promising donor materials for solution processed SM BHJ solar cells. Quinquethiophenes (**O5T**) were proved to have deeper HOMO level than septithiophenes for the decreased conjugations,[26] therefore higher open circuit voltage (V_{oc}) could be expected to obtain for **O5T** derivatives. In addition, A-D-A molecules based on quinquethiophenes have been investigated by Bäuerle and co-workers,[27–31] and vacuum-processed solar cell with PCE of 6.9%[30] was achieved recently for **DCV5T** derivatives. Considering the above factors and our previous work, we herein wish to report the synthesis and characterization of three **O5T** derivatives with different end groups (**DCAO5T**, **DERHD5T** and **DIN5T**, as shown in Scheme 1) for solution processed BHJ solar cells. Among them, **DERHD5T** shows V_{oc} as high as 1.08 volt and power conversion efficiency of 4.63% under AM 1.5G irradiation (100 mW cm^{-2}), **DCAO5T** and **DIN5T** showed PCE of 3.27% and 4.00%, V_{oc} of 0.88 V and 0.78 V, respectively. Theoretical investigation was carried to understand their different performance and the results are in consistent with the experimental data.

G. Long, Dr. X. Wan, B. Kan, Dr. Y. Liu, G. He, Z. Li, Y. Zhang, Q. Zhang, Prof. Y. Chen
Key Laboratory of Functional Polymer Materials and Centre of Nanoscale Science and Technology
Institute of Polymer Chemistry
College of Chemistry
Nankai University
Tianjin, 300071, China
E-mail: xjwan@nankai.edu.cn; yschen99@nankai.edu.cn
Y. W. Zhang, Dr. M. Zhang
College of Chemistry
Nankai University
300071, Tianjin, China

DOI: 10.1002/aenm.201300046

2. Results and Discussion

2.1. Synthesis

The synthesis of **DCAO5T**, **DERHD5T** and **DIN5T** are shown in **Figure 2** with details described in the Experimental Section. Compound **DFO5T** (diformyl quinquethiophene) was prepared following the literature method.[26] By the Knoevenagel condensation of compound **DFO5T** with octyl 2-cyanoacetate (**CAO**), 3-ethylrhodanine (**ERHD**) and 2*H*-indene-1,3-dione (**IN**), **DCAO5T**, **DERHD5T** and **DIN5T** were afforded with high yields.

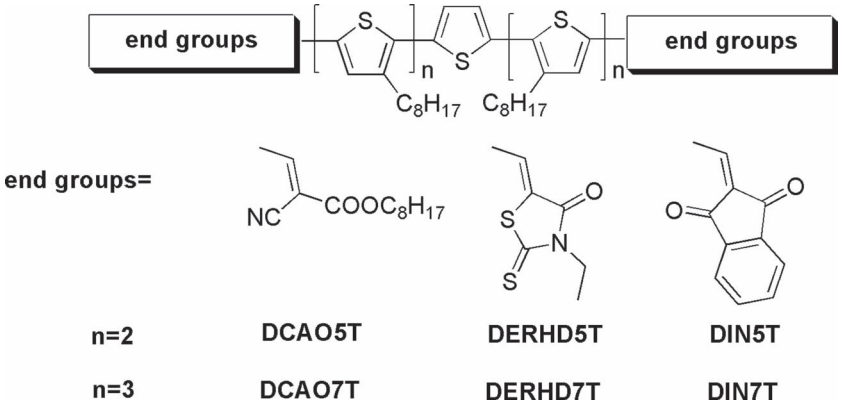

Figure 1. Chemical structure of quinquethiophene and septithiophene derivatives with different end groups.

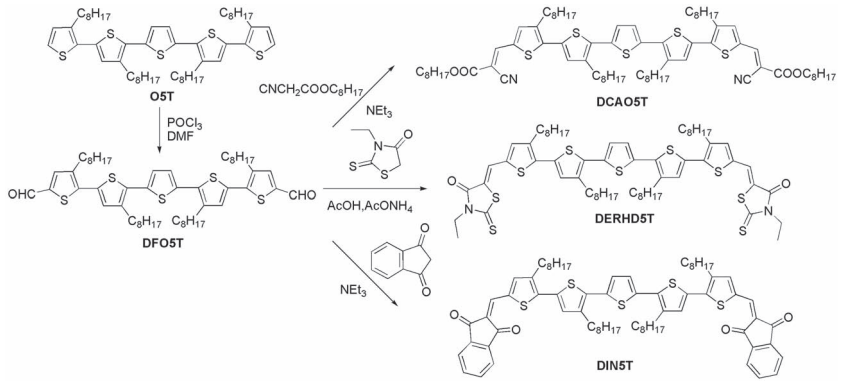

Figure 2. Synthesis route of **DCAO5T**, **DERHD5T** and **DIN5T**.

2.2. Thermal Properties

The thermal stability of these compounds was investigated by thermal gravimetric analysis (TGA) at a heating rate of 10 °C/min under N_2 (**Figure 3**). **Table 1** lists 5% weight loss temperatures (T_d) of these compounds determined from TGA curves. The results reveal that the onset decomposition temperatures of the compounds are all around 360 °C, which indicates that they are quite thermally stable and can be used for device fabrication.

2.3. Optical Properties

UV-Vis absorption spectra of **DCAO5T**, **DERHD5T** and **DIN5T** in chloroform are shown in **Figure 4** and summarized in Table 1. Compared with the model compound **O5T** (λ_{max} = 385 nm), the absorption peaks of these three A-D-A **O5T** derivatives exhibited about 100 to 150 nm red shift for the strong intramolecular charge transfer (ICT) from the conjugated backbone to the end electron-withdrawing units. With different acceptor strength of **CAO**, **ERHD** and **IN** groups, the absorption peaks for **DCAO5T**, **DERHD5T** and **DIN5T** are at 489, 508 and 541 nm, respectively. **DIN5T** shows larger molar absorption coefficient of 6.94×10^4 L mol^{-1} cm^{-1} than **DERHD5T** (5.54×10^4 L mol^{-1} cm^{-1}) and **DCAO5T** (4.34×10^4 L mol^{-1} cm^{-1}), which is in the similar trend with the calculated transition dipole moments (μ_{tr}). The absorption spectra of these compounds in the film state show an obvious broadening and red shift of the bands compared with the solution spectra. In addition, three compound films all exist shoulder peaks, especially for **DERHD5T** and **DIN5T**, indicating planar conjugated backbone and stronger π–π interactions in the film state. As shown in Table 1, the solution and film optical band gaps are decreased from **DCAO5T**, **DERHD5T** to **DIN5T**, which is in consistent with the CV and DFT calculation[32] results (Table S1) shown below.

2.4. Electrochemical Characterization

The electrochemical properties of **DCAO5T**, **DERHD5T** and **DIN5T** were investigated by cyclic voltammetry (CV).[33] The potentials were internally calibrated using the ferrocene/ferrocenium of the (Fc/Fc^+) redox couple (4.8 eV below the vacuum level). As shown in Figure S1 to S3, the CV of **DCAO5T**, **DERHD5T** and **DIN5T** in CH_2Cl_2 solution have two reversible oxidation waves and one irreversible reduction wave. The energy levels of the HOMO and LUMO were calculated from the onset oxidation potential and the onset reduction potential, which are −5.25 and −3.23 eV for **DCAO5T**, −5.09 and −3.20 eV for **DERHD5T**, and −5.11 and −3.36 eV for **DIN5T**. Among these three compounds, **DCAO5T** shows the deepest HOMO level and **DIN5T** has the deepest LUMO level. **DCAO5T** and **DERHD5T** have similar LUMO level, while **DERHD5T** and **DIN5T** exhibit almost the same HOMO level. The electrochemical band gap is in the same order of **DCAO5T>DERHD5T>DIN5T** with

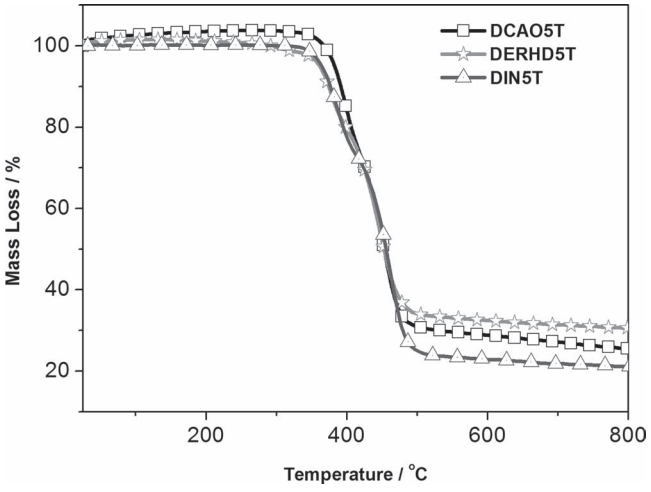

Figure 3. TGA curve of **DCAO5T**, **DRHD5T**, and **DIN5T** determined with a scanning rate of 10 °C/min under N_2.

Table 1. Optical, electrochemical and thermal stability data for **O5T** derivatives.

	solution			film				CV			T_d [°C]
	$\lambda_{max,sol}$ [nm]	$E_{g,opt}$ [eV]	ε [L/mol/cm]	$\lambda_{max,film}$ [nm]	$E_{g,opt,film}$ [eV]	ε [cm^{-1}]	IP_{UPS} [eV]	HOMO [eV]	LUMO [eV]	$E_{g,CV}$ [eV]	
DCAO5T	490	2.08	4.34×10^4	561	1.80	3.91×10^4	5.87	−5.25	−3.23	2.02	382
DERHD5T	509	2.01	5.54×10^4	615,671	1.65	4.66×10^4	5.66	−5.09	−3.20	1.89	361
DIN5T	541	1.91	6.94×10^4	622,680	1.56	4.91×10^4	5.83	−5.11	−3.36	1.75	364

the optical band gap. The ionization energy (IP) of **DCAO5T**, **DERHD5T** and **DIN5T** has been determined to be 5.87, 5.66 and 5.83 eV by ultraviolet photoelectron spectroscopy (UPS),[20] respectively. These values are comparable to the results of **DCV5T** derivatives (5.6 ± 0.1 eV).[28] The difference of the solution CV and solid state UPS results may be ascribed to the aggregation from solution to film states.[25]

These electrochemical and optical data demonstrated that the band gap and absorption spectra of these quinquethiophenes derivatives can be tuned effectively through the introduction of different acceptor terminal units as we discussed previously,[34] and the strength of these acceptor units is in the order of **IN**>**ERHD**>**CAO**.

2.6. Hole Mobility

The hole mobility of the pristine **DCAO5T**, **DERHD5T** and **DIN5T** was measured by the space charge limited current (SCLC) method.[35,36] As plotted in Figure S4, **DCAO5T**, **DERHD5T** and **DIN5T** show hole mobility values of 3.94×10^{-4}, 3.86×10^{-4} and 5.51×10^{-4} cm^2 V^{-1} s^{-1}, respectively, which are in the same order of magnitude with their **O7T** analogues. The hole mobility of **DERHD5T** increases to 5.76×10^{-4} cm^2 V^{-1} s^{-1} after thermal annealing at 110 °C for 10 min, while thermal annealing treatment does not work for **DCAO5T** and **DIN5T.**

2.7. X-ray Diffraction

To investigate the structural ordering of **DCAO5T**, **DERHD5T** and **DIN5T** in the solid state, we performed XRD analysis for thin films spin-coated from $CHCl_3$ solution onto glass substrates and detailed *d*-spacing values are summarized in **Table 2**. As shown in Figure S5, all the three conjugated molecules exhibit strong (100) reflection peaks at $2\theta = 4.02°$ for **DCAO5T**, 4.78° for **DERHD5T** and 4.98° for **DIN5T**, corresponding to d_{100}–spacing values of 21.98, 18.47 and 17.73 Å, respectively. These d_{100}–spacing values are the distance between the planes of the main conjugation chains of these molecules separated by alkyl side chains. The second-order diffraction peaks (200) for **DCAO5T** and **DERHD5T** (after annealing) were also observed, implying a highly organized assembly of these conjugated molecules at solid state. Moreover, the planar structure was supported by the calculation result using density functional theory (DFT) with the B3LYP/6-31G* model[37,38] (Figure S6). The difference of the *d*-spacing values and the peak intensity indicate that the organization of these films can be tuned by using different end groups of these molecules, which could have impact on their morphology and thus device performance discussed below.

XRD patterns of the neat films could give a rough estimation about the crystal domain size (*D*) using the Scherrer equation.[30] The crystal size of **DCAO5T**, **DERHD5T** and **DIN5T** are 42.82, 37.19 and 24.64 nm before annealing, which increase to 47.73, 47.78 and 55.94 nm after thermal annealing at 110 °C for 10 min. After incorporating with $PC_{61}BM$, the crystal size for **DCAO5T** and **DIN5T** decrease to 30.41 nm and 22.34 nm, and no obvious change was observed after thermal annealing. However the crystal size of **DERHD5T** increases to 111.0 nm when mixed with $PC_{61}BM$, which decreases dramatically to 41.9 nm after thermal annealing. This could be the critical reason for the increased PCE after thermal annealing for **DERHD5T** based solar cell as discussed in the following section.

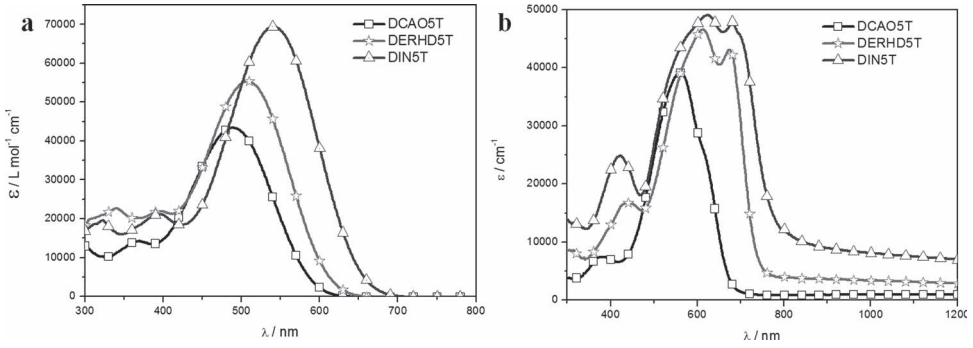

Figure 4. UV-Vis absorption spectra of three **O5T** derivatives in chloroform (a) and as-cast film (b).

Table 2. *d*-spacing and estimated crystal domain sizes (*D*) of the conjugated molecules with and without $PC_{61}BM$ before and after thermal annealing.

	annealing[a]	(100)				(200)
		2θ [°]	d_{100} [Å]	FWHM[b] [°]	*D* [nm]	d_{200}/Å [Å]
DCAO5T	No	4.02	21.98	0.184	42.82	10.99
	Yes	4.02	21.96	0.165	47.73	10.93
DERHD5T	No	4.78	18.47	0.212	37.19	–
	Yes	4.80	18.39	0.165	47.78	9.18
DIN5T	No	4.98	17.73	0.320	24.64	–
	Yes	5.08	17.38	0.141	55.94	–
DCAO5T:$PC_{61}BM$ (1:0.75)	No	3.98	22.18	0.259	30.41	–
	Yes	4.00	22.07	0.282	27.93	–
DERHD5T:$PC_{61}BM$ (1:0.5)	No	4.72	18.71	0.071	111.02	–
	Yes	4.84	18.24	0.188	41.94	–
DIN5T:$PC_{61}BM$ (1:0.5)	No	5.04	17.52	0.353	22.34	–
	Yes	4.66	18.95	0.306	25.76	–

[a]thermal annealing at 110 °C for 10 min; [b]FWHM (Full Width Half Maximum).

2.8. Fabrication and Characterization of O5T derivatives based Organic Solar Cells

2.8.1. OPV Performance

The photovoltaic properties of **DCAO5T**, **DERHD5T** and **DIN5T** based BHJ devices with the standard sandwich structure ITO/PEDOT:PSS/donor:$PC_{61}BM$/LiF/Al was explored using the simple solution process from $CHCl_3$ solution. Device optimizations results data were presented in the Supporting Information (Table S2). **Figure 5** presents typical *J*–*V* curve of different donor:$PC_{61}BM$ (w:w) BHJ films processed from chloroform under AM 1.5G illumination. For **DCAO5T**, the optimal performance was obtained from the device with the active layer comprised of a blend of **DCAO5T** and $PC_{61}BM$ with a weight ratio of 1:0.75, which gave a V_{oc} of 0.88 V, a J_{sc} of 7.02 mA cm^{-2}, a *FF* of 0.53 and a PCE of 3.27%. For **DIN5T**, the optimal BHJ device showed V_{oc} = 0.78 V, J_{sc} = 8.13 mA cm^{-2}, *FF* = 0.63 and PCE of 4.00%. Device based on the **DERHD5T**:$PC_{61}BM$(1:0.5, w:w) blend showed a V_{oc} of 1.06 V, a J_{sc} of 5.34 mA cm^{-2}, a *FF* of 0.33 and a PCE of 1.87%, the PCE increased to 3.64%, with V_{oc} of 1.08 V, J_{sc} of 7.84 mA cm^{-2}, *FF* of 0.43 after thermal annealing at 110 °C for 10 min. However, the thermal annealing treatment does not work for **DCAO5T** and **DIN5T**.

Table 3. Summary of device performance for BHJ solar cell based on the **O5T** derivatives.

Donor:$PC_{61}BM$ (w:w)	V_{oc} [V]	J_{sc} [mA cm^{-2}]	*FF*	PCE [%]
DCAO5T:$PC_{61}BM$ (1:0.75)[a]	0.88	7.02	0.53	3.27
DERHD5T:$PC_{61}BM$ (1:0.5)[a]	1.06	5.34	0.33	1.87
DERHD5T:$PC_{61}BM$ (1:0.5)[a,b]	1.08	7.84	0.43	3.64
DIN5T:$PC_{61}BM$ (1:0.5)[a]	0.78	8.13	0.63	4.00
DCAO5T:$PC_{61}BM$ (1:0.75)[c]	0.82	5.92	0.56	2.72
DERHD5T:$PC_{61}BM$ (1:0.5)[b,c]	1.02	9.26	0.49	4.63
DIN5T:$PC_{61}BM$ (1:0.5)[c]	0.80	7.81	0.61	3.81

[a]LiF/Al; [b]thermal annealing at 110 °C for 10 min; [c]Ca/Al.

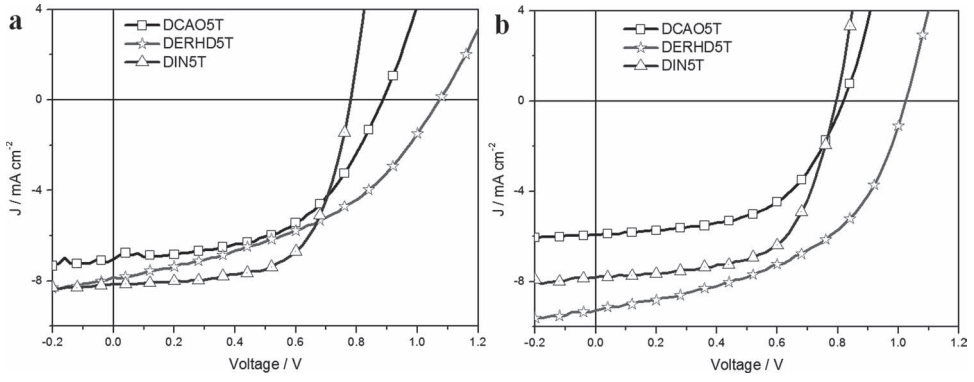

Figure 5. *J*–*V* curves of BHJ solar cells prepared from **DCAO5T**, **DERHD5T** and **DIN5T** blend with $PC_{61}BM$ using LiF/Al (a) and Ca/Al (b) as the cathode.

Table 4. Measured and simulated performance parameters for oligothiophene derivatives and P3HT.

	ratio	$J_{0,n}$	nkT/q	J_{so}	$V_{oc,cal}$	$V_{oc,exp}$
	[w:w]	[mA cm^{-2}]		[mA cm^{-2}]	[V]	[V]
DCAO5T[a)]	1:0.75	1.60×10^{-8}	0.0540	4.16×10^{-3}	1.06	0.88
DERHD5T[a)]	1:0.5	1.15×10^{-9}	0.0550	5.99×10^{-5}	1.24	1.08
DIN5T[a)]	1:0.5	4.92×10^{-8}	0.0451	3.52×10^{-2}	0.85	0.78
DCAO7T[b)]	1:0.5	1.34×10^{-10}	0.0382	1.31×10^{-3}	0.96	0.86
DERHD7T[a)]	1:0.5	3.86×10^{-11}	0.0389	5.41×10^{-5}	1.04	0.92
DIN7T[b)]	1:1	1.56×10^{-6}	0.0541	3.11×10^{-2}	0.84	0.78
P3HT[b)]	1:1	2.56×10^{-6}	0.0400	2.87×10^{1}	0.60	0.57

[a)]LiF/Al; [b)]Ca/Al is used as the cathode, OPV data for DCAO7T, DERHD7T and DIN7T from ref [24], ref [25] and ref [54].

During our optimization process, Ca/Al instead of LiF/Al as the cathode was also investigated. The devices of **DCAO5T** and **DIN5T** with $PC_{61}BM$ with the same ratio displayed lower PCEs of 2.72% and 3.81% than those values using LiF/Al cathode. However, the device of **DERHD5T**/$PC_{61}BM$ with the ratio of 1: 0.5 displayed a significantly improved PCE to 4.63% with a V_{oc} of 1.02 V, J_{sc} of 9.26 mA cm^{-2} and *FF* of 0.49 after thermal annealing at 110 °C for 10 min. Also, no clear improvement was observed by thermal annealing for **DCAO5T** and **DIN5T**. The optimized thickness for **DCAO5T**, **DERHD5T** and **DIN5T** with $PC_{61}BM$ is ca. 105, 100 and 115 nm, respectively, and the EQE spectra are shown in Figure S7.

Furthermore, similar devices using [6, 6]-phenyl-C_{71}-butyric acid methyl ester ($PC_{71}BM$) as the acceptor were also fabricated and tested. Though intensive optimization has been performed, generally lower PCEs and J_{sc} were obtained, which might be due to poor miscibility with $PC_{71}BM$ as observed in the AFM images.[39] This is also consistent with our previous small molecules with septithiophene main chain.[23–25,34]

2.8.2. Discussion About the Open Circuit Voltage

From the most widely accepted concept that V_{oc} is mainly determined by the energy difference between the HOMO of the donor and the LUMO of the acceptor materials under ohmic contact.[40] According to the CV results in Table 1, **DCAO5T** is expected to exhibit the highest V_{oc} and **DERHD5T** would give the lowest V_{oc} among these three compounds. However the experimental results were totally opposite, **DERHD5T** demonstrates V_{oc} over 1 volt. To our knowledge, only very few compounds including polymers have been reported with V_{oc} over 1 volt for solution processed BHJ solar cells.[41–49] Meanwhile, **DIN5T** shows the smallest V_{oc} of 0.78 V. The V_{oc} of **DCAO5T** is in the middle of the above two compounds with value of 0.88 V.

It has been reported that the electronic coupling (or intermolecular interaction) between the donor and acceptor has great influence the reverse dark saturation current density and thus the V_{oc}.[50–52] Reducing the electronic coupling or intermolecular interaction between the donor and acceptor can reduce the reverse dark saturation current density and thus improve the V_{oc}. In the following part, we wish to employ the reported theoretical method to explain our experimental results. According to Koen Vandewal's work, the dark injected current J_{inj} versus applied voltage[53] for donor:fullerene devices was exponentially fitted according to Equation 1,[52] therefore to determine reverse saturation current density $J_{0,n}$. The detailed fitting range and plots were shown in Figure S8.

$$J_{inj} = J_{0,n} \exp\left(\frac{qV}{nk_BT}\right) \quad (1)$$

$$J_{0,n} = J_{so} \exp\left(\frac{-\Delta E_{DA}}{2nk_BT}\right) \quad (2)$$

Then based on the CV results of ΔE_{DA} (the energy difference between the HOMO of the donor and the LUMO of the acceptor materials), the magnitude of the pre-exponential term, J_{so} was obtained (Equation 2), which is related to the intermolecular overlap at the D/A interface that determine the carrier generation/recombination rate, independent of ΔE_{DA}.[51,52] Since the studied oligomers have the identical quinquethiophenes backbone with the only difference of the end groups, J_{so} is believed to represent the strength of intermolecular interactions in the donor/acceptor blends predominately affected by the end groups. Then the V_{oc} was calculated from the Equation 3[50] which is simplified and further solved from Shockley equation at the open circuit conditions based on the of assume of low series resistance and high shunt resistance.

$$V_{oc,cal} = \frac{nk_BT}{q} \ln\left(\frac{J_{sc}}{J_{0,n}} + 1\right) \approx \frac{nk_BT}{q} \ln\left(\frac{J_{sc}}{J_{so}}\right) + \frac{\Delta E_{DA}}{2q} \quad (3)$$

As shown in **Table 4**, J_{so} is in the order of **DERHD5T**<**DCAO5T**<**DIN5T**. Similar trend is also obtained based on the ΔE_{DA} from UPS results [**DERHD5T** (2.71×10^{-4} mA cm^{-2})<**DCAO5T** (3.32×10^{-2} mA cm^{-2})<**DIN5T** (1.16 mA cm^{-2})]. Among these three compounds, **DERHD5T** showed the weakest interaction with $PC_{61}BM$, therefore the largest V_{oc}. Based on the optimized structure of **DERHD5T**, the two ethyl groups on the rhodanine unit are arranged on the two sides of the **O5T** plane (Figure S9), which may decrease the distance with $PC_{61}BM$, therefore weaken the interactions with the acceptor from the view point of steric hindrance.[51] With different end groups on the quinquethiophenes backbone, the

change of dipole moment can be expected to affect the packing arrangement of the molecules in the solid state and thus indirectly impact on the electronic couplings with the acceptor, therefore acted on the open circuit voltage.[14] The correlation between the experimental V_{oc} and calculated ground state dipole moment plot for **O5T** derivatives is shown in Figure S10.

For comparison, the calculated $V_{oc,cal}$ for **O7T** derivatives and P3HT (poly[3-hexylthiophene]) were also carried out and summarized in Table 4, which was in consistent with the trend of the experimental V_{oc}.

2.8.3. Atomic Force Microscopy

In order to understand the effect of morphology of the active layers impact on their OPV device performance, the surface morphology of blend film of pristine and mixture of **DCAO5T**, **DERHD5T** or **DIN5T** with $PC_{61}BM$ spin-coated from $CHCl_3$ solutions was studied by tapping-mode AFM, and the topography images are shown in Figure S11. The pristine donor films have different crystalline domain size and various root mean square (*rms*) roughness, which is 2.11 nm for **DCAO5T**, 6.77 nm for **DERHD5T** and 5.01 nm for **DIN5T**. As shown in Figure S11 (a-d), the phase images of the blend film reveal two distinct feature types, which were assigned to the acceptor $PC_{61}BM$-rich and donor-rich domains. This is quite different from that of pristine donor films. The *rms* roughness of blend films is 2.75, 0.58 and 3.05 nm for **DCAO5T**/$PC_{61}BM$, **DERHD5T**/$PC_{61}BM$ and **DIN5T**/$PC_{61}BM$ films, respectively. After thermal annealing at 110 °C for 10 min, the *rms* roughness for **DERHD5T** neat film decreased to 6.19 nm, while **DERHD5T**/$PC_{61}BM$ increased a little to 0.93 nm. From the above AFM data, it is clearly that **DERHD5T** shows much better miscibility with $PC_{61}BM$ than the other two compounds.[15]

3. Conclusions

Three **O5T** derivatives with different end groups with acceptor strength of **IN>ERHD>CAO** were synthesized and characterized. BHJ solar cells based on these donors with $PC_{61}BM$ were fabricated and higher V_{oc} (1.08 V) than their septithiophene analogs were obtained. Among three molecules, **DERHD5T** exhibited highest V_{oc} over 1 volt and PCE of 4.63%. Besides the deeper HOMO, weaker interaction with $PC_{61}BM$ is believed to be the main reason for the increased V_{oc} based on analyzing the reverse saturation current density and optimized molecular structure. Future work would focus to decrease not only the HOMO level of donor material, but also the interactions between donor and acceptor materials to increase V_{oc}.

4. Experimental Section

Instrument and Measurements: NMR spectra were taken on a Bruker AV400 Spectrometer. High resolution MALDI spectra were collected with a Fourier transform-ion cyclotron resonance mass spectrometer instrument (Varian 7.0T FTICR-MS). The thermogravimetric analyses (TGA) and differential scanning calorimetry (DSC) analyses studies were carried out on a NETZSCH STA 409PC instrument under purified nitrogen gas flow with a 10 °C min^{-1} heating rate. The temperature of degradation (T_d) corresponds to a 5% weight loss. UV-Vis spectra were obtained with a JASCO V-570 spectrophotometer. The organic molecule films on quartz used for absorption spectral measurement were prepared by spin-coating their chloroform solutions. XRD experiments were performed on a Rigaku D/max-2500 X-ray diffractometer with Cu-Kα radiation (k = 1.5406 Å) at a generator voltage of 40 kV and a current of 100 mA. Atomic force microscope (AFM) investigation was performed using Bruker MultiMode 8 in "tapping" mode. Cyclic voltammetry (CV) experiments were performed with a LK98B II Microcomputer-based Electrochemical Analyzer in CH_2Cl_2 solutions. All measurements were carried out at room temperature with a conventional three-electrode configuration employing a glassy carbon electrode as the working electrode, a saturated calomel electrode (SCE) as the reference electrode, and a Pt wire as the counter electrode. Dichloromethane was distilled from calcium hydride under dry nitrogen immediately prior to use. Tetrabutylammonium phosphorus hexafluoride (Bu_4NPF_6, 0.1 M) in dichloromethane was used as the supporting electrolyte, and the scan rate was 100 mV s^{-1}, HOMO and LUMO levels were estimated relative to the energy level of a ferrocene reference (4.8 eV below vacuum level). External quantum efficiency (EQE) values of the encapsulated devices were measured using a lock-in amplifier (SR810, Stanford Research Systems). The devices were illuminated by monochromatic light from a 150 W xenon lamp passing through an optical chopper and a monochromator. Photon flux was determined by a calibrated standard silicon photodiode. For ultraviolet photoelectron spectroscopy (UPS) measurements, a 30 nm thick PEDOT:PSS film was coated on a pre-cleaned Si substrates with 40nm SiO_2. Chloroform solutions of **O5T** derivatives (10 mg/mL) were then spin coated at speeds of 1500 rpm with thickness about 100 nm. The UPS measurements (Thermo ESCALAB 250) were carried out using the He I ($h\nu$ = 21.2 eV) source. During UPS measurements, a sample bias of -8 V was used in order to separate the sample and the secondary edge for the analyzer. In order to confirm reproducibility of UPS spectra, we repeated these measurements twice on a set of samples.

Quantum Chemical Calculations: The geometry structure of the three molecules were optimized by using DFT calculations (B3LYP/6-31G*), and the frequency analysis was followed to assure that the optimized structures were stable states.

Device fabrication and photovoltaic characterization: Hole mobility was measured using a diode configuration of ITO/PEDOT:PSS/donor/Al by taking dark current in the range of 0-6 V and fitting the results to a space charge limited form, where the space charge limited current (SCLC) is described by Equation 4[35,36]:

$$J^{\frac{1}{2}} = \left(\frac{9\varepsilon_0\varepsilon_r\mu_h}{8L^3}\right)^{\frac{1}{2}}\cdot(V_{appl}-V_{bi}-V_r) = kV_{appl} - kC$$
$$k = \left(\frac{9\varepsilon_0\varepsilon_r\mu_h}{8L^3}\right)^{\frac{1}{2}}; C = V_{bi}+V_r \quad (4)$$

where J is the current density, L is the film thickness of active layer, μ_h is the hole mobility, ε_r is the relative dielectric constant of the transport medium, ε_0 is the permittivity of free space (8.85×10^{-12} F m^{-1}), V is the internal voltage in the device and $V = V_{appl} - V_{bi} - V_r$, where V_{appl} is the applied voltage to the device, V_r is the voltage drop due to contact resistance and series resistance across the electrodes, and V_{bi} is the built-in voltage due to the relative work function difference of the two electrodes.

The photovoltaic devices were fabricated with a structure of glass/ITO/PEDOT:PSS/donor:acceptor/LiF or Ca/Al. The ITO-coated glass substrates were cleaned by ultrasonic treatment in detergent, deionized water, acetone, and isopropyl alcohol under ultrasonication for 15 minutes each and subsequently dried by a nitrogen blow. A thin layer of PEDOT:PSS (Baytron P VP AI 4083, filtered at 0.45 μm) was spin-coated (3000 rpm, ca. 30 nm thick) onto ITO surface. After being baked at 150 °C for 20 min, the substrates were transferred into an argon-filled glove box. Subsequently, the active layer was spin-casted from different blend ratios (weight-to-weight) of donor (8 mg mL^{-1})

and $PC_{61}BM/PC_{71}BM$ in chloroform solution at 1500 rpm for 20 sec on the ITO/PEDOT:PSS substrate. Thermal annealing was performed at 110 °C for 10 minutes if it is necessary. The active layer thickness was measured using a Dektak 150 profilometer. Finally, 1 nm LiF or 20 nm Ca layer and 80 nm Al layer were deposited on the active layer under high vacuum ($< 3 \times 10^{-4}$ Pa). The effective area of each cell was 4 mm^2 defined by masks for all the solar cell devices discussed in this work.

The current density-voltage (*J–V*) curves of photovoltaic devices were obtained by a Keithley 2400 source-measure unit. The photocurrent was measured under illumination simulated 100 mW cm^{-2} AM 1.5G irradiation using a xenon-lamp-based solar simulator [Oriel 96000 (AM 1.5G)] in an argon filled glove box. Simulator irradiance was calibrated using a certified silicon diode.

Materials: Octyl 2-cyanoacetate, 2-ethylrhodanine and 2*H*-indene-1,3-dione were purchased from J&K Scientific, Alfa Asear and HEOWNS, respectively, and used without further purification. Compound **DFO5T** (diformyl quinquethiophene) was prepared following the literature method.[26]

*Synthesis of **DIN5T***: Diformylquinquethiophene (**DFO5T**, 1.29 g, 1.41 mmol) was dissolved in a solution of 2*H*-indene-1,3-dione (2.06 g, 14.06 mmol) in dry $CHCl_3$ (125 mL) and then ten drops of triethylaminewere added and the resulting solution was stirred overnight, under argon, at room temperature. The reaction mixture was poured into methanol to obtain precipitate, which was collected by filtration and washed with methanol and dried. After removal of solvent it was chromatographied on silica gel using chloroform/petrolium (4:1) as eluant to afford **DIN5T** as a brown solid, which was further dissolved in small amount of $CHCl_3$, and added dropwise to hexane to obtain reprecipitate. Then the residue was dried under vacuum and affording a brown solid powder. (871.1 mg, 52.8% yield). M.p.: 204.4 °C. ^{1}H NMR (400 MHz, $CDCl_3$, δ) 7.97 (t, J = 6.78, 4H), 7.89 (s, 2H), 7.79-7.77 (m, 6H), 7.32 (s, 2H), 7.18 (s, 2H), 2.86 (q, J = 6.61 Hz, 8H), 1.74 (td, J = 15.16, 7.65, 7.65 Hz, 8H), 1.45-1.30 (m, 40H), 0.89 (t, J = 6.40Hz, 12H). ^{13}C NMR (100 MHz, $CDCl_3$, δ) 190.41, 189.80, 145.54, 145.00, 142.03, 140.80, 140.67, 140.52, 135.92, 135.74, 134.97, 134.76, 134.52, 133.20, 130.88, 126.54, 123.71, 122.95, 122.76, 31.93, 31.89, 31.60, 30.61, 30.10, 29.71, 29.57, 29.50, 29.43, 29.39, 29.34, 29.29, 22.70, 14.14. HRMS (MALDI-FTICR, *m/z*): calcd for $C_{72}H_{84}O_4S_5$ $[M]^+$, 1172.4973; found 1172.4965

*Synthesis of **DCAO5T***: **DCAO5T** was prepared from **DFO5T** with a method similar to that described earlier for **DIN5T**. Yield: 80%. M.p. 140.1°C. ^{1}H NMR (400 MHz, $CDCl_3$, δ) 8.20 (s, 2H), 7.56 (s, 2H), 7.20 (s, 2H), 7.15 (s, 2H), 4.29 (t, J = 6.7 Hz, 4H), 2.82 (m, 8H), 1.71 (m. 12H), 1.28-1.43 (m, 60H), 0.88 (t, 18H). ^{13}C NMR (100 MHz, $CDCl_3$, δ) 163.15, 146.02, 141.74, 140.99, 140.68, 140.51, 135.81, 132.99, 132.88, 132.59, 130.90, 126.63, 116.04, 97.68, 66.57, 31.90, 31.87, 31.79, 30.61, 30.18, 29.65, 29.49, 29.45, 29.38, 29.31, 29.25, 29.19, 29.16, 28.58, 25.82, 22.68, 22.66, 14.11. HRMS (MALDI-FTICR, *m/z*): calcd for $C_{76}H_{110}N_2O_4S_5$ $[M]^+$, 1274.7069; found 1274.7068.

*Synthesis of **DERHD5T***: DFO5T (250 mg, 0.272 mmol) was dispersed in a solution of AcOH (120 mL). 3-Ethylrhodanine (800 mg, 4.97 mmol) and then $AcONH_4$ (1.5 g, 19.46 mmol) were added subsequently and the resulting solution was refluxed and stirred for 12 hours, under argon, at room temperature. The reaction mixture was then extracted with CH_2Cl_2, washed with water and dried over Na_2SO_4. After removal of solvent it was chromatographied on silica gel using a mixture of dichloromethane and petroleum ether (1:1) as eluant to afford **DERHD5T** as a dark brown solid with metallic luster. (262 mg, 80% yield). M.p. 156.3 °C. ^{1}H NMR (300 MHz, $CDCl_3$, δ) 7.78 (s, 2H), 7.22 (s, 2H), 7.15 (s, 2H), 7.12 (s, 2H), 4.19 (q, J = 7.06, 7.04, 7.04 Hz, 4H), 2.80 (t, 6H), 1.70 (m, 8H), 1.43-1.26 (m, 48H), 0.88 (t, J = 6.55 Hz, 12H). ^{13}C NMR (100 MHz, $CDCl_3$, δ) 192.08, 167.33, 141.13, 141.12, 140.53, 140.52, 139.59, 137.42, 135.80, 135.78, 135.13, 132.97, 132.24, 132.22, 129.95, 126.46, 124.95, 120.56, 39.94, 31.91, 30.61, 30.25, 29.67, 29.66, 29.52, 29.51, 29.42, 29.35, 29.29, 22.70, 14.13, 12.32. HRMS (MALDI-FTICR, *m/z*): calcd for $C_{64}H_{86}N_2O_2S_9$ $[M]^+$, 1202.4176; found 1202.4172.

Supporting Information

Supporting Information is available from the Wiley Online Library or from the author.

Acknowledgements

The authors gratefully acknowledge financial support from the NSFC (Grants 50933003, 50902073 51273093 and 50903044), MOST (Grants 2012CB933401, and 2011DFB50300) and NSF of Tianjin City (Grant 10ZCGHHZ00600). Supporting Information is available online from Wiley InterScience or from the author.

Received: January 13, 2013
Published online: March 13, 2013

[1] Y. J. Cheng, S. H. Yang, C. S. Hsu, *Chem. Rev.* **2009**, *109*, 5868.
[2] P. M. Beaujuge, J. M. J. Fréchet, *J. Am. Chem. Soc.* **2011**, *133*, 20009.
[3] H. Zhou, L. Yang, W. You, *Macromolecules* **2012**, *45*, 607.
[4] B. Walker, C. Kim, T. Q. Nguyen, *Chem. Mater.* **2011**, *23*, 470.
[5] A. Mishra, P. Bäuerle, *Angew. Chem. Int. Ed.* **2012**, *51*, 2020.
[6] Y. Lin, Y. Li, X. Zhan, *Chem. Soc. Rev.* **2012**, *41*, 4245.
[7] Z. He, C. Zhong, S. Su, M. Xu, H. Wu, Y. Cao, *Nat. Photon.* **2012**, *6*, 593.
[8] U. Mayerhöffer, K. Deing, K. Gruβ, H. Braunschweig, K. Meerholz, F. Würthner, *Angew. Chem. Int. Ed.* **2009**, *48*, 8776.
[9] S. Loser, H. Miyauchi, J. W. Hennek, J. Smith, C. Huang, A. Facchetti, T. J. Marks, *Chem. Commun.* **2012**, *48*, 8511.
[10] J. Mei, K. R. Graham, R. Stalder, J. R. Reynolds, *Org. Lett.* **2010**, *12*, 660.
[11] G. Wei, S. Wang, K. Sun, M. E. Thompson, S. R. Forrest, *Adv. Energy Mater.* **2011**, *1*, 184.
[12] T. Rousseau, A. Cravino, E. Ripaud, P. Leriche, S. Rihn, A. De Nicola, R. Ziessel, J. Roncali, *Chem. Commun.* **2010**, *46*, 5082.
[13] X. Zhao, C. Piliego, B. Kim, D. A. Poulsen, B. Ma, D. A. Unruh, J. M. J. Fréchet, *Chem. Mater.* **2010**, *22*, 2325.
[14] D. Demeter, T. Rousseau, P. Leriche, T. Cauchy, R. Po, J. Roncali, *Adv. Funct. Mater.* **2011**, *21*, 4379.
[15] J. Liu, B. Walker, A. Tamayo, Y. Zhang, T. Q. Nguyen, *Adv. Funct. Mater.* **2013**, *23*, 47.
[16] H. Shang, H. Fan, Y. Liu, W. Hu, Y. Li, X. Zhan, *Adv. Mater.* **2011**, *23*, 1554.
[17] J. Shin, N. S. Kang, K. H. Kim, T. W. Lee, J. I. Jin, M. Kim, K. Lee, B. K. Ju, J. M. Hong, D. H. Choi, *Chem. Commun.* **2012**, *48*, 8490.
[18] O. P. Lee, A. T. Yiu, P. M. Beaujuge, C. H. Woo, T. W. Holcombe, J. E. Millstone, J. D. Douglas, M. S. Chen, J. M. Fréchet, *Adv. Mater.* **2011**, *23*, 5359.
[19] J. Zhou, X. Wan, Y. Liu, Y. Zuo, Z. Li, G. He, G. Long, W. Ni, C. Li, X. C. Su, Y. Chen, *J. Am. Chem. Soc.* **2012**, *134*, 16345
[20] C. J. Takacs, Y. Sun, G. C. Welch, L. A. Perez, X. Liu, W. Wen, G. C. Bazan, A. J. Heeger, *J. Am. Chem. Soc.* **2012**, *134*, 16597.
[21] T. S. van der Poll, J. A. Love, T. Q. Nguyen, G. C. Bazan, *Adv. Mater.* **2012**, *24*, 3646.
[22] A. Mishra, C. Q. Ma, P. Bäuerle, *Chem. Rev.* **2009**, *109*, 1141.
[23] Y. S. Liu, X. J. Wan, B. Yin, J. Y. Zhou, G. K. Long, S. G. Yin, Y. S. Chen, *J. Mater. Chem.* **2010**, *20*, 2464.
[24] Y. S. Liu, X. J. Wan, F. Wang, J. Y. Zhou, G. K. Long, J. G. Tian, J. B. You, Y. Yang, Y. S. Chen, *Adv. Energy Mater.* **2011**, *1*, 771.
[25] Z. Li, G. R. He, X. J. Wan, Y. S. Liu, J. Y. Zhou, G. K. Long, Y. Zuo, M. T. Zhang, Y. S. Chen, *Adv. Energy Mater.* **2012**, *2*, 74.
[26] Y. S. Liu, J. Y. Zhou, X. J. Wan, Y. S. Chen, *Tetrahedron* **2009**, *65*, 5209.

[27] K. Schulze, M. Riede, E. Brier, E. Reinold, P. Bäuerle, K. Leo, *J. Appl. Phys.* **2008**, *104*, 074511.
[28] K. Schulze, C. Uhrich, R. Schüppel, K. Leo, M. Pfeiffer, E. Brier, E. Reinold, P. Bäuerle, *Adv. Mater.* **2006**, *18*, 2872.
[29] A. Mishra, C. Uhrich, E. Reinold, M. Pfeiffer, P. Bäuerle, *Adv. Energy Mater.* **2011**, *1*, 265.
[30] R. Fitzner, E. Mena-Osteritz, A. Mishra, G. Schulz, E. Reinold, M. Weil, C. Körner, H. Ziehlke, C. Elschner, K. Leo, M. Riede, M. Pfeiffer, C. Uhrich, P. Bäuerle, *J. Am. Chem. Soc.* **2012**, *134*, 11064.
[31] R. Fitzner, E. Reinold, A. Mishra, E. Mena-Osteritz, H. Ziehlke, C. Körner, K. Leo, M. Riede, M. Weil, O. Tsaryova, A. Weiβ, C. Uhrich, M. Pfeiffer, P. Bäuerle, *Adv. Funct. Mater.* **2011**, *21*, 897.
[32] Gaussian 09, Revision B.01, Gaussian, Inc., Wallingford CT, 2010, see Supporting Information for full citation.
[33] Y. F. Li, Y. Cao, J. Gao, D. L. Wang, G. Yu, A. J. Heeger, *Syn. Met.* **1999**, *99*, 243.
[34] G. R. He, Z. Li, X. J. Wan, Y. S. Liu, J. Y. Zhou, G. K. Long, M. T. Zhang, Y. S. Chen, *J. Mater. Chem.* **2012**, *22*, 9173.
[35] V. D. Mihailetchi, L. J. A. Koster, P. W. M. Blom, C. Melzer, B. de Boer, J. K. J. van Duren, R. A. J. Janssen, *Adv. Funct. Mater.* **2005**, *15*, 795.
[36] Z. Chiguvare, V. Dyakonov, *Phys. Rev. B* **2004**, *70*, 235207.
[37] C. Lee, W. Yang, R. G. Parr, *Phys. Rev. B* **1988**, *37*, 785.
[38] A. Becke, *J. Chem. Phys.* **1993**, *98*, 5648.
[39] Z. F. Ma, E. G. Wang, K. Vandewal, M. R. Andersson, F. L. Zhang, *Appl. Phys. Lett.* **2011**, *99*, 143302.
[40] M. C. Scharber, D. Mühlbacher, M. Koppe, P. Denk, C. Waldauf, A. J. Heeger, C. J. Brabec, *Adv. Mater.* **2006**, *18*, 789.
[41] M. Mastalerz, V. Fischer, C. Q. Ma, R. A. Janssen, P. Bäuerle, *Org. Lett.* **2009**, *11*, 4500.
[42] M. Svensson, F. L. Zhang, S. C. Veenstra, W. J. H. Verhees, J. C. Hummelen, J. M. Kroon, O. Inganäs, M. R. Andersson, *Adv. Mater.* **2003**, *15*, 988.
[43] A. Gadisa, W. Mammo, L. Andersson, S. Admassie, F. Zhang, M. R. Andersson, O. Inganäs, *Adv. Funct. Mater.* **2007**, *17*, 3836.
[44] W. W. Wong, C. Q. Ma, W. Pisula, C. Yan, X. Feng, D. J. Jones, K. Müllen, R. A. Janssen, P. Bäuerle, A. B. Holmes, *Chem. Mater.* **2010**, *22*, 457.
[45] E. Ripaud, T. Rousseau, P. Leriche, J. Roncali, *Adv. Energy Mater.* **2011**, *1*, 540.
[46] F. Brunetti, X. Gong, M. Tong, A. Heeger, F. Wudl, *Angew. Chem. Int. Ed.* **2010**, *49*, 532.
[47] J. Yuan, Z. Zhai, H. Dong, J. Li, Z. Jiang, Y. Li, W. Ma, *Adv. Funct. Mater.* **2013**, *23*, 885.
[48] H. Buerckstuemmer, E. V. Tulyakova, M. Deppisch, M. R. Lenze, N. M. Kronenberg, M. Gsaenger, M. Stolte, K. Meerholz, F. Wüerthner, *Angew. Chem. Int. Ed.* **2011**, *50*, 11628.
[49] R. Schueppel, K. Schmidt, C. Uhrich, K. Schulze, D. Wynands, J. Brédas, E. Brier, E. Reinold, H. Bu, P. Baeuerle, B. Maennig, M. Pfeiffer, K. Leo, *Phys. Rev. B* **2008**, *77*, 085311.
[50] M. D. Perez, C. Borek, S. R. Forrest, M. E. Thompson, *J. Am. Chem. Soc.* **2009**, *131*, 9281.
[51] L. Yang, H. Zhou, W. You, *J. Phys. Chem. C* **2010**, *114*, 16793.
[52] K. Vandewal, K. Tvingstedt, A. Gadisa, O. Inganäs, J. V. Manca, *Nat. Mater.* **2009**, *8*, 904.
[53] A. Kumar, S. Sista, Y. Yang, *J. Appl. Phys.* **2009**, *105*, 094512.
[54] G. R. He, Z. Li, X. J. Wan, J. Y. Zhou, G. K. Long, M. T. Zhang, Y. S. Chen, *J. Mater. Chem. A* **2013**, *1*, 1801.